J. Biochem. **137**, 273–285 (2005)
DOI: 10.1093/jb/mvi040

Mutation Study of Antithrombin: The Roles of Disulfide Bonds in Intracellular Accumulation and Formation of Russell Body–Like Structures

Yuki Tanaka[1], Kazue Ueda[1], Tetsuo Ozawa[2], Isao Kitajima[2], Shoji Okamura[1], Masashi Morita[1], Sadaki Yokota[3] and Tsuneo Imanaka[1,*]

[1]Department of Biological Chemistry, Faculty of Pharmaceutical Sciences, and [2]Department of Clinical and Laboratory Medicine, Faculty of Medicine, Toyama Medical and Pharmaceutical University, 2630 Sugitani, Toyama 930-0194; and [3]Biological Laboratory, Faculty of Medicine, University of Yamanashi, 1100 Shimokatou, Tamaho, Yamanashi 409-3898

Received October 8, 2004; accepted December 7, 2004

Antithrombin (AT) is a major plasma protease inhibitor with three intramolecular disulfide bonds and a deficiency of it is associated with venous thrombosis. Recently, we prepared CHO cells overexpressing a novel mutant, AT(C95R), with a disulfide bond removed, and revealed that this mutant remained for a long time in the endoplasmic reticulum (ER) without being degraded and also accumulated in newly formed membrane structures that resembled Russell bodies (RB) [Tanaka, Y. *et al.* (2002) *J. Biol. Chem.* 277, 51058–51067]. In this study, we replaced each of the individual cysteine residues of AT with an arginine and also two paired cysteine residues with arginines. We stably expressed these mutant ATs in CHO cells, and examined the roles of each cysteine residue or disulfide bond in the accumulation of mutant ATs and the formation of RB-like structures. In pulse-chase experiments, the secretion of mutant ATs with single mutations decreased ~1/5–1/50 times compared to that of the wild type AT. All of the mutant ATs were retained in the ER and were also found to accumulate in the RB-like structures. On the other hand, the fates of mutant ATs with double mutations fell into two categories. Secretion of mutant AT(C8R,C128R) decreased only ~1/2 times and no RB-like structures appeared. Mutants AT(C21R,C95R) and AT(C247R,C430R) exhibited similar secretion kinetics to the mutant ATs with the single mutations and were found in RB-like structures. On a sucrose gradient, all of the mutant ATs that induced RB-like structures migrated as oligomeric structures, whereas wild type AT and AT(C8R,C128R) migrated as monomers. Further, to clarify the morphological pathway through which RB-like structures are formed, we prepared CHO cells in which the expression of AT(C95R) was controlled by the Tet-On system. During expression of AT(C95R), RB-like structures formed through expansion of the ER. These results suggest that the correct folding with each disulfide bond is essential for the secretion of AT and oligomerization of mutant ATs in the ER is involved in the formation of RB-like structures.

Key words: antithrombin, disulfide bond, endoplasmic reticulum, protein folding, Russell body.

Abbreviations: AT, antithrombin; DSP, dithiobis(succinimidyl propionate); ER, endoplasmic reticulum; ERAD, endoplasmic reticulum–associated degradation; PBS, phosphate-buffered saline; RB, Russell body(ies); UPR, unfolded protein response.

Antithrombin (AT) is the major plasma inhibitor of thrombin and other activated coagulation factors, and is important for the maintenance of normal hemostasis by means of its prevention of activated coagulation reactions (*1*, *2*). Human AT contains four glycosylation sites at asparagine residues 96, 135, 155, and 192, and three intramolecular disulfide bonds between cysteine residues 8–128, 21–95, and 247–430 (*3*, *4*). AT is synthesized by hepatocytes as a precursor that carries a 32–amino acid signal peptide. After cotranslational cleavage of the signal peptide and maturation of oligosaccharide chains, mature AT of 432 amino acid residues with a molecular mass of 58 kDa is secreted into the plasma (*5*, *6*). AT has two functional domains; an N-terminal heparin-binding domain and a C-terminal protease-binding domain which includes the reactive site (*7*, *8*). The intramolecular disulfide bonds and processing of oligosaccharide chains are both thought to be important for the correct folding of the nascent AT polypeptide. Naturally occurring mutations in the AT gene can lead to inherited AT deficiencies, which are highly associated with familial venous thromboembolic diseases (*9*). Among the AT deficiency variants, type I is only found in heterozygous patients, and is characterized by reduction of the immunological and

*To whom correspondence should be addressed. Tel: +81-76-434-7545, Fax: +81-76-434-4656, E-mail: imanaka@ms.toyama-mpu.ac.jp

Table 1. **Oligonucleotide primer sequences used for the generation of mutant AT constructs.**

Construct name	Forward primer (5′ to 3′) (top) Reverse primer (5′ to 3′) (bottom)
AT (C95G)	TATGACCAAGCTGGGTGCCGGTAATGACACC
	GGTGTCATTACCGGCACCCAGCTTGGTCATA
AT (C95S)	TATGACCAAGCTGGGTGCCAGTAATGACACC
	GGTGTCATTACTGGCACCCAGCTTGGTCATA
AT (C8R)	TGTGGACATCCGCACAGCCAAGCCGCGG
	CCGCGGCTTGGCTGTGCGGATGTCCACA
AT (C128R)	GCCAAACTGAACCGCCGACTCTATCGAAAAGCC
	GCCTTTTCGATAGAGTCGGCGGTTCAGTTTGGC
AT (C247R)	TGATGGAGAGTCGCGTTCAGCATCTATGATGTAC
	GTACATCATAGATGCTGAACGCGACTCTCCATCA
AT (C430R)	GGGCAGAGTAGCCAACCCTCGTGTTAAGTAAAATG
	CATTTTACTTAACACGAGGGTTGGCTACTCTGCCC

The underlined letters indicate the single base mutation leading to amino acid replacement of glycine, serine or arginine.

functional AT levels to ~50% of normal. Intracellular degradation of mutant ATs is thought to be one of the reasons for type I AT deficiency (*10*).

The major site for quality control within the secretory pathway is the endoplasmic reticulum (ER). Within the ER, newly synthesized secretory polypeptides are associated with resident chaperone proteins until they are fully folded and covalently modified with oligosaccharides. Once the polypeptides are correctly folded, they move toward ER-exit sites and are packed into ER-to-Golgi complex transport vesicles (*11–13*). Most proteins that fail to retain the correct conformation in the ER have been shown to be retrotranslocated to the cytoplasm and degraded through ER-associated degradation (ERAD) by proteasomes (*14–16*). In the case of AT mutations, two different forms of AT, AT(ΔE313) and AT(P429Stop), are degraded through ERAD in BHK cells overexpressing the mutant ATs (*17*). *N*-Linked oligosaccharide processing has also been shown to affect ERAD of the mutant ATs (*18*).

Relocation of misfolded proteins from the ER to the cytoplasm is a critical step for the proper disposal of the proteins. Failure of proper relocation leads to the accumulation of proteins in the ER lumen. The proteins often exist as aggregates and are thought to be sorted into Russell bodies (RB) (*19*). RB were originally observed in plasma cells that synthesized mutant IgM (*20*, *21*). Similar structures have been reported in the hepatocytes of an individual carrying mutant α1-antitrypsin alleles (PiZ; the glutamic acid at position 342 being substituted by lysine) and transgenic mice (*22–24*), and in yeast expressing a mutant form of an aspartic protease from *Rhizopus niveus* (*25*). RB are thought to be derived from dilated ER cisternae containing condensed misfolded proteins, resulting in exclusion of aggregates composed of misfolded proteins (*19*). However, the intracellular fate of the misfolded proteins and the pathway of RB formation have been poorly characterized to date.

Recently, we found a novel missense mutation, AT *Morioka* (C95R), which causes the loss of one of the three disulfide bonds (*26*), and reported that this mutant AT is not transported to the Golgi apparatus but rather accumulates without degradation in novel structures surrounded by a single membrane derived from the ER that resemble RB (*27*). In this study, we replaced each of the individual and paired cysteine residues of AT, stably expressed the mutant ATs in CHO cells, and studied the roles of each cysteine residue or disulfide bond in the accumulation of mutant AT in the ER as well as the formation of RB-like structures. Further, we studied the time course of RB formation using CHO cells in which AT synthesis was controlled by the Tet-On system.

EXPERIMENTAL PROCEDURES

Materials—PRO-MIX™: L-[^{35}S] *in vitro* Cell Labeling Mix (70% L-[^{35}S]methionine and 30% L-[^{35}S]cysteine, >37 TBq/mmol) and ECL+Plus, a Western blotting detection system, were purchased from Amersham Biosciences (Piscataway, NJ). pTRE2hyg, the CHO-K1 Tet-On cell line, hygromycin B, and doxycycline were obtained from BD Biosciences Clontech (Franklin Lake, NJ). Rabbit anti–human AT antibodies, mouse anti-KDEL antibodies, rabbit anti–rat BiP antibodies, and rabbit anti–canine calnexin antibodies were obtained from Athens Research, Technology, Inc. (Athens, GA), Calbiochem-Novabiochem (San Diego, CA), Affinity BioReagents, (Golden, CO), and StressGen Biotechnologies Corp. (Victoria, Canada), respectively. Dithiobis(succinimidyl propionate) (DSP) was from Pierce (Rockford, IL). Protein A–Sepharose CL-4B, a molecular weight marker for sucrose gradient centrifugation, and L-glutamine, L-cysteine, and L-methionine were from Sigma (St. Louis, MO). Trans Fast™ and geneticine disulfate (G418) were purchased from Promega (Madison, MI), and the Effectene transfection reagents were from Qiagen (Valencia, CA). Phenylmetylsulfonyl fluoride was purchased from Wako Pure Chemicals (Osaka, Japan). Antipain, chymostatin, leupeptin, and pepstatin A were from Peptide Institute Inc. (Osaka, Japan).

Construction of Mutant AT cDNAs—The expression vectors of pcDNA3.1(+)/AT, AT(C95R), and AT(C21R,C95R) are described elsewhere (*27*). Mutant versions of AT containing mutations C95G and C95S were constructed with a Quick Change™ site-directed mutagenesis kit (Stratagene) with pcDNA 3.1(+)/AT as the template, and desig-

nated as pcDNA3.1(+)/AT(C95G) and AT(C95S), respectively. The oligonucleotide primers used are listed in Table 1. Other mutant versions of AT with single or double mutations of cysteine residues, C8R, C21R, C128R, C247R, and C430R, were also constructed using pcDNA 3.1(+)/AT as the template by site-directed mutagenesis, and designated as pcDNA3.1(+)/AT(C8R), AT(C21R), AT(C128R), AT(C247R), and AT(C430R), respectively. AT(C8R,C128R) and AT(C247R,C430R) were constructed using pcDNA 3.1(+)/AT(C8R) or AT(C247R) as templates, and designated pcDNA3.1(+)/AT(C8R,C128R) and AT(C247R,C430R), respectively. To prepare a gene expression vector with the Tet-On system, pcDNA3.1(+)/AT or AT(C95R) was excised with the *Bam*HI and *Sal*I sites, and then ligated into pTRE2hyg at the corresponding sites, pTRE2hyg/AT or AT(C95R) being thus obtained. The mutations in the constructions were confirmed by DNA sequencing with an ABI 310 DNA sequencer (Perkin Elmer Life Science, Wellesley, MA).

Cell Culture and Transient Expression—CHO cells were cultured in Ham's F-12 medium containing 10% (v/v) fetal calf serum at 37°C under 5% CO_2 as described previously (*27*, *28*). For transient expression, 5×10^5 cells were seeded onto 6-well plates, cultured at 37°C for 18 h, and then transfected with 5.0 μg of pcDNA3.1(+)/AT, AT(C95R), AT(C95S), or AT(C95G), which had been mixed with Trans Fast™ according to the manufacturer's instructions. Two days after the transfection, the cells were used for a pulse-chase study following the procedures described below.

Establishment of Stable Cell Lines—To prepare CHO cells overexpressing the mutant ATs, cells were transfected with 3.2 μg of mutant AT cDNAs cloned into pcDNA3.1(+), which had been mixed with Effectene transfection reagents. The procedure was essentially the same as previously described (*27*, *28*). In addition, to prepare CHO cells in which expression of the wild type or mutant AT(C95R) is controlled by doxycycline, CHO cells expressing reverse Tet repressor protein (rTerR) were transfected with 3.0 μg of wild type or mutant AT(C95R) cDNA cloned into pTRE2hyg, which had been mixed with Effectene transfection reagents. In the case of the CHO-K1 Tet-On cell line, the cells were cultured in DMEM containing 10% (v/v) fetal calf serum, 100 μg/ml of G418, and 100 μg/ml of hygromycin. The surviving 5–10 colonies were removed by the cylinder technique and subjected to immunoblot analysis of AT.

Pulse-Chase Experiments—CHO cells were plated at a concentration of 2×10^5 onto 6-well plates and cultured at 37°C for 18 h in Ham's F-12 medium containing 10% (v/v) fetal calf serum. The culture medium was removed and the cells were washed 3 times with phosphate-buffered saline (PBS). The cells were then incubated in methionine-free medium at 37°C for 1 h, pulse-labeled d for 1 h with 925 kBq of [^{35}S]methionine and cysteine, and then incubated for various periods in Ham's F-12 medium containing 2 mM methionine and 2 mM cysteine (0–9 h). After each step, the culture medium was removed and the cells were harvested in 0.25 M sucrose containing 1 mM EDTA, 0.1% (v/v) ethanol, and 5 mM Hepes, pH 7.4. To avoid proteolytic breakdown, antipain, chymostatin, leupeptin, and pepstatin A (each at a final concentration of 10 μg/ml), and phenylmethylsulfonyl fluoride (at a final concentration of 100 μg/ml) were added. ^{35}S-AT in the medium and cell fractions was immunoprecipitated with rabbit anti–human AT antibodies as previously described (*27*). The immunoprecipitates were subjected to SDS-PAGE. The gels were dried and the bands of AT were quantified with a Fuji BAS 5000 imaging analyzer (Fuji Film).

Electron Microscopy—For transmission electron microscopy, CHO cells were fixed with 4% (w/v) paraformaldehyde, 2% (w/v) glutaraldehyde in 0.1 M cacodylate hydrochloride, pH 7.4, for 1 h at room temperature and then washed with PBS as described previously (*27*). Cells were then detached from the culture dishes with 20% ethanol and enclosed in low melting temperature agarose. Cell pellets were postfixed for 1 h with 2% reduced osmium and then embedded in Epon (*29*). Thin sections were mounted on copper grids, and then stained with uranyl acetate and lead citrate. All thin sections were examined under a Hitachi H600 electron microscope at an acceleration voltage of 75 kV. For immunoelectron microscopy, CHO cells were fixed with 4% (w/v) paraformaldehyde, 0.2% (w/v) glutaraldehyde in 0.1 M Hepes buffer, pH 7.4, for 1 h at room temperature. After being washed with PBS, the cells were dehydrated with a graded dimethylformamide series at –20°C and then embedded in LR White. Polymerization of the resin was performed under UV light at –20°C for 24 h. Thin sections were cut with an Ultracut R microtome equipped with a diamond knife (Reichert, Germany). AT and ER resident proteins were visualized with the combination of rabbit anti–human AT antibodies and mouse anti-KDEL antibodies, respectively, and a 10-nm protein A–gold probe (*28*, *29*).

Sucrose Density Gradient Centrifugation—CHO cells were grown in 100-mm dishes, washed with PBS, collected, and then allowed to stand in PBS in the presence of 1 mM DSP for 30 min at 4°C as described previously (*30*). DSP was then inactivated by the addition of 50 mM glycine in PBS. The cells were lysed in 1 ml of 0.25 M sucrose, 10 mM Hepes, pH 7.6, 150 mM NaCl, 2 mM EDTA, 0.2% Triton X-100 containing antipain, chymostatin, leupeptin, and pepstatin A (each at a final concentration of 10 μg/ml), and phenylmethylsulfonyl fluoride (at a final concentration of 100 μg/ml), and then incubated with rotation for 30 min at 4°C. Then, the lysates were centrifuged at $600 \times g$ for 10 min. The supernatant fractions were each subjected to density centrifugation in a 10 ml linear sucrose gradient [10–50% (w/v)] in a NVT65 rotor (Beckman, Fullerton, CA). The gradient was rested on 0.5 ml of 80% (w/v) sucrose. All solutions contained 10 mM Hepes, pH 7.6, 150 mM NaCl, 2 mM EDTA and 0.2% Triton X-100. Centrifugation was carried out at $165{,}000 \times g$ for 2 h at 4°C. Fractions of approximately 1.0 ml were collected from the bottom of the tube and the density of each fraction was determined by refractometry. Each sample was separated by SDS-PAGE and then subjected to immunoblot analysis.

Other Methods—Protein was assayed as described previously (*27*). Immunoblotting was performed according to the procedure of Kashiwayama *et al*. using ECL+Plus, a Western blotting detection system (*31*).

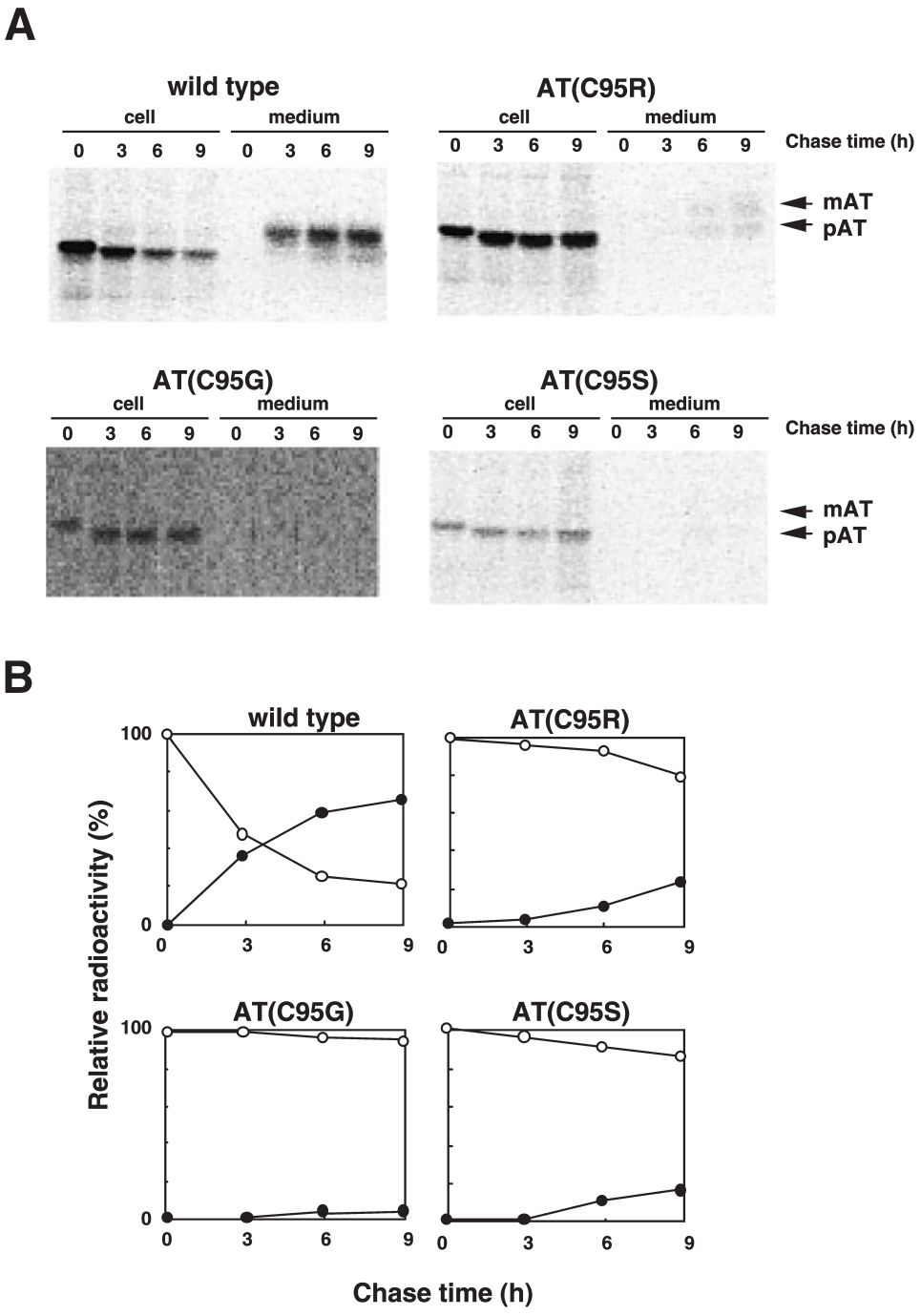

Fig. 1. **Pulse-chase analysis of newly synthesized AT in cells and medium prepared from CHO cells transiently expressing the wild type or mutant ATs (C95R, C95G and C95S).** Cells were transfected with the wild type AT or a mutant AT cDNA. After 2 d, the cells were pulse-labeled with [^{35}S]methionine and cysteine for 1 h. Duplicate cultures were harvested at the times indicated, and AT was examined following immunoprecipitation and SDS-PAGE. The amount of AT was determined with a BAS 5000 imaging analyzer. A, CHO cells transfected with wild type AT or mutant ATs. The arrows indicate the positions of mature AT (mAT) and premature AT (pAT), respectively. B, kinetics of intracellular transport and secretion of AT after pulse-chase labeling. The open circles represent the amount of radiolabeled AT in the cells, and the closed circles represent the amount in the medium.

RESULTS

Replacement of the Cysteine Residue at Position 95 with Serine or Glycine—Previously, we demonstrated that a novel missense mutation named AT *Morioka* (C95R), which results in the loss of one disulfide bond, accumulated in cells without degradation (*27*). In this study, we first examined whether or not replacement of this cysteine residue with arginine was essential for the intracellular accumulation of the mutant AT. We constructed a mutant cDNA in which cysteine residue 95 was substituted with glycine or serine and then conducted a pulse-chase study using CHO cells transiently expressing one of the mutant ATs. The cells expressing the wild or mutant ATs were labeled for 1 h with [^{35}S]methionine and cysteine, and then the radioactivity was chased for up to 9 h. As shown in Fig. 1, the newly synthesized wild type AT was secreted into the medium with a half-life of ~3 h. In contrast, mutant ATs, AT(C95G) and AT(C95S) as well as AT(C95R) were not secreted into the medium up to 3 h and only very small amounts of the mutant ATs were secreted into the medium in the chase period of 9 h. These results suggest that mutation of the cysteine residue is essential for the intracellular accumulation of mutant AT.

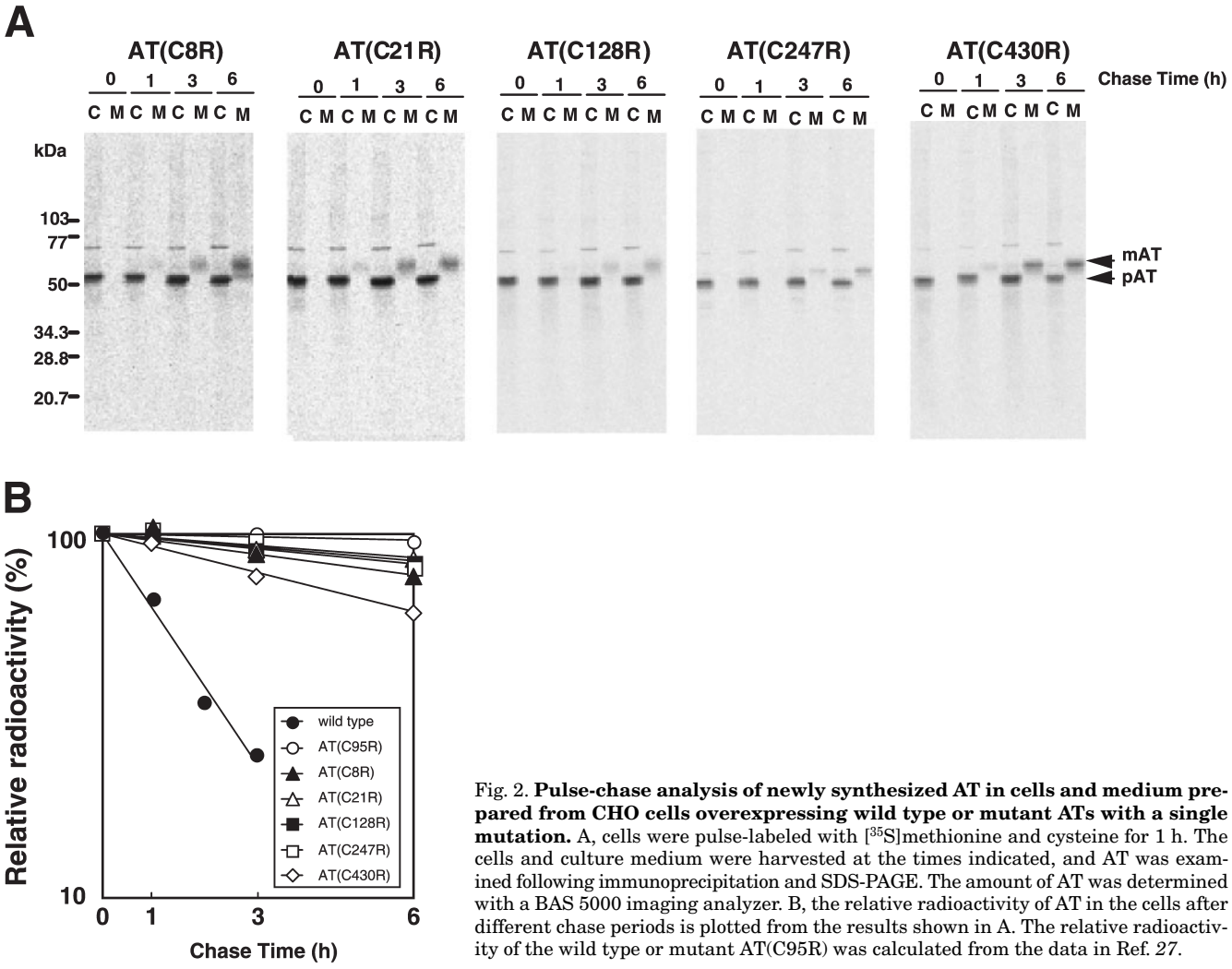

Fig. 2. **Pulse-chase analysis of newly synthesized AT in cells and medium prepared from CHO cells overexpressing wild type or mutant ATs with a single mutation.** A, cells were pulse-labeled with [^{35}S]methionine and cysteine for 1 h. The cells and culture medium were harvested at the times indicated, and AT was examined following immunoprecipitation and SDS-PAGE. The amount of AT was determined with a BAS 5000 imaging analyzer. B, the relative radioactivity of AT in the cells after different chase periods is plotted from the results shown in A. The relative radioactivity of the wild type or mutant AT(C95R) was calculated from the data in Ref. *27*.

Intracellular Transport of a Mutant AT with Single or Double Mutation of Cysteine Residues—Previously, using CHO cells overexpressing wild type AT, we demonstrated that newly synthesized wild type AT was secreted into the medium with a half-life of ~1.5 h. In contrast, most mutant AT(C95R) was retained in the cells without degradation and was secreted about 50 times more slowly into the medium (*27*). To examine the intracellular transport of other mutant ATs with single or double mutations of cysteine residues, we prepared CHO cells expressing mutant ATs, AT(C8R), AT(C21R), AT(C128R), AT(C247R) and AT(C430R), obtained by replacing each cysteine residue with an arginine, and further prepared CHO cells expressing mutant ATs, AT(C8R,C128R) and AT(C247R,C430R), obtained by replacing pairs of cysteine residues with arginines. Although the expression of mutant ATs in the cells varied among the cells prepared (Figs. 2A and 3A), the expression of mutants AT(C95R) and AT(C21R,C95R) in the previous study was roughly equal to that of AT(C21R) and AT(C247R,C430R), respectively.

First, we examined the intracellular transport of mutant ATs with single mutation of cysteine residues. CHO cells expressing each mutant AT were labeled for 1 h with [^{35}S]methionine and cysteine, and then the radioactivity was chased for up to 6 h. As shown in Fig. 2A, all of the mutant ATs were secreted very slowly into the medium in the chase period of 6 h. More than 80% of newly synthesized mutant ATs was retained in the cells and their molecular masses were 52 kDa, corresponding to that of premature AT with high-mannose type oligosaccharides (*27*), suggesting that they were not transported to the Golgi apparatus and did not bear complex oligosaccharides, as in the case of mutant AT(C95R) (*27*). Quantification of the radioactivity was performed with a BAS 5000 imaging analyzer, which revealed that total AT radioactivity remained almost constant throughout the chase period. As shown in Fig. 2B, intracellular AT decreased following first-order kinetics, and the rates of decrease of mutant ATs in the cells (in other words, the rates of secretion of mutant ATs) were ~5–50 times lower than that of the wild type AT.

Concerning double mutation of cysteine residues involved in disulfide bond formation, we demonstrated previously that mutant AT(C21R,C95R) was secreted faster than mutant AT(C95R) (*27*). We had, therefore, expected that other mutants, AT(C8R,C128R) and AT(C247R,C430R), would be secreted faster than mutant ATs with single mutations of the corresponding cysteine residues. However, the fates of these mutant ATs fell into two categories. As expected, in the CHO cells expressing

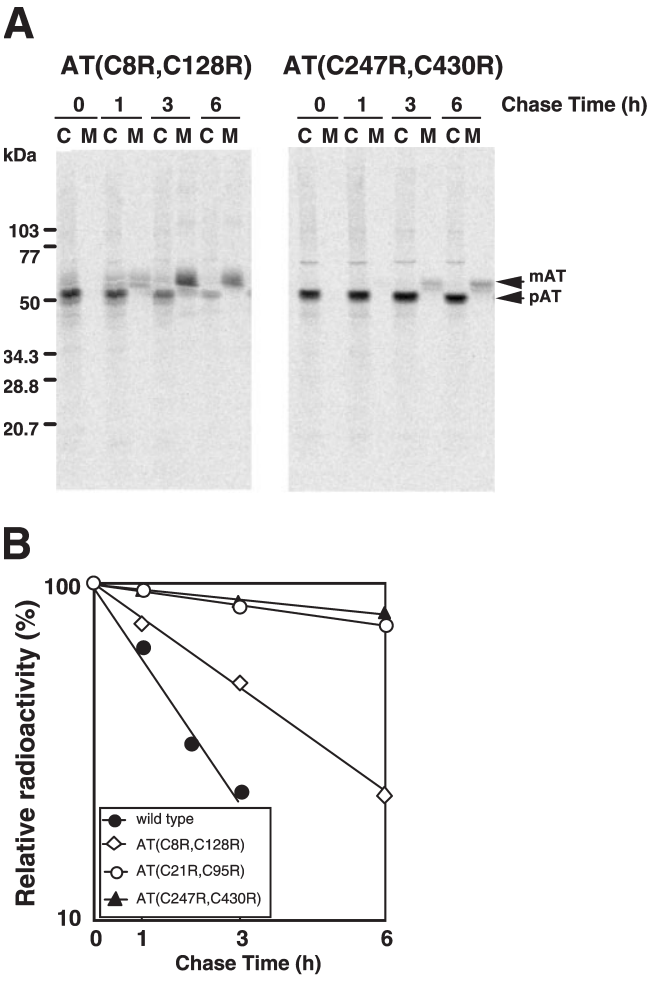

Fig. 3. **Pulse-chase analysis of newly synthesized AT in cells and medium prepared from CHO cells overexpressing mutant ATs with a double mutation.** A, cells were pulse-labeled with [^{35}S]methionine and cysteine for 1 h. The cells and culture medium were harvested at the times indicated, and AT was examined following immunoprecipitation and SDS-PAGE. B, the relative radioactivity of AT in the cells after different chase periods was plotted from the results shown in A. The relative radioactivity of mutant AT(C21R,C95R) was calculated from the data in Ref. *27*.

mutant AT(C8R,C128R) the secretion rate increased by ~15 times compared with those of the corresponding single mutants, AT(C8R) and AT(C128R) (Fig. 3). In contrast, secretion of mutant AT(C247R,C430R) did not increase compared with that of mutants AT(C247R) and AT(C430R) and the secretion rate was still ~20 times lower than that of the wild type AT (Fig. 3). Although secretion rates were different among the mutations, most of the intracellular ATs exhibited a molecular mass of ~52 kDa, suggesting that the mutant ATs possess a high-mannose-type oligosaccharide and that the site of accumulation is the ER.

Subcellular Localization of Mutant ATs—To examine the relationship between the accumulation of mutant ATs and the formation of RB-like structures, the localization of mutant ATs in CHO cells was analyzed by immunoelectron microscopy. As shown in Fig. 4, a large number of gold particles corresponding to mutant ATs were observed in variously sized structures surrounded by a single membrane in CHO cells overexpressing mutant ATs with single mutations. The structures resembled those found in CHO cells overexpressing mutant AT(C95R) (*27*) and were different from any subcellular organelles. As shown in Fig. 5, in the cells expressing AT(C21R,C95R) and AT(C247R,C430R), many gold particles were also observed in variously sized structures surrounded by a membrane. The structures in CHO cells expressing AT(C247R,C430R) were spherical, whereas those in CHO cells expressing AT(C21R,C95R) were narrow and tubular. We also examined the subcellular localization of ER-resident proteins bearing the KDEL sequence using anti-KDEL antibodies. As shown in Fig. 5, many gold particles against the ER-resident proteins were also detected in the RB-like structures. On the other hand, mutant AT(C8R,C128R) seems to be located in small vesicles corresponding to intermediate vesicles in the secretory pathway that was demonstrated in CHO cells overexpressing the wild type AT (*27*).

Molecular Sizes of Mutant ATs on a Sucrose Gradient—The mutant ATs remained for a long time in the ER without degradation, suggesting that the mutant ATs form aggregates and/or associate with ER-resident proteins to prevent their retrograde transport. In the previous study, we showed that mutant AT(C95R) is associated with chaperone BiP (*27*). To determine the molecular sizes of the mutant ATs, we prepared cell lysates in the presence of DSP, and the sizes were determined by density gradient centrifugation on 10–50% linear sucrose gradients. As shown in Fig. 6, wild type AT and mutant AT(C8R,C128R), which did not form RB-like structures, were mostly recovered in the fractions corresponding to an approximate molecular mass of 66 kDa, suggesting that these ATs exist as a monomeric form in the ER. On the other hand, the peak fraction of other mutant ATs, *i.e.* AT(C95R), AT(C8R), AT(C21R), AT(C128R), and AT(C21R,C95R), were heavy ones corresponding heterogeneous populations with molecular masses of between 66–670 kDa. Mutants AT(C247R), AT(C430R), and AT(C247R,C430R) existed as larger complexes and a part of them was recovered in the bottom fraction of the gradient. These results suggest that oligomerization of mutant ATs causes decreases in the secretion rates of the mutant ATs and induces the formation of RB-like structures. In addition, the association of wild type AT and mutant AT(C8R,C128R) with BiP was not detected on co-immunoprecipitation under the conditions where the association of mutant AT(C95R) with BiP was detected (data not shown).

Time course of Appearance of RB-Like Structures—To clarify the morphological pathway by which RB-like structures are formed, we prepared CHO cells in which the expression of wild type AT and mutant AT(C95R) was controlled by the Tet-On system. The synthesis of wild type and mutant AT(C95R) was started by the addition of doxycycline, and the time course of AT expression as well as the appearance of RB-like structures were examined by immunoblotting and electron microscopy, respectively. As shown in Fig. 7, the amount of mutant AT(C95R) in the cells increased during incubation with doxycycline. After incubation for 36 h, the content of mutant AT(C95R) became almost equal to that in CHO cells sta-

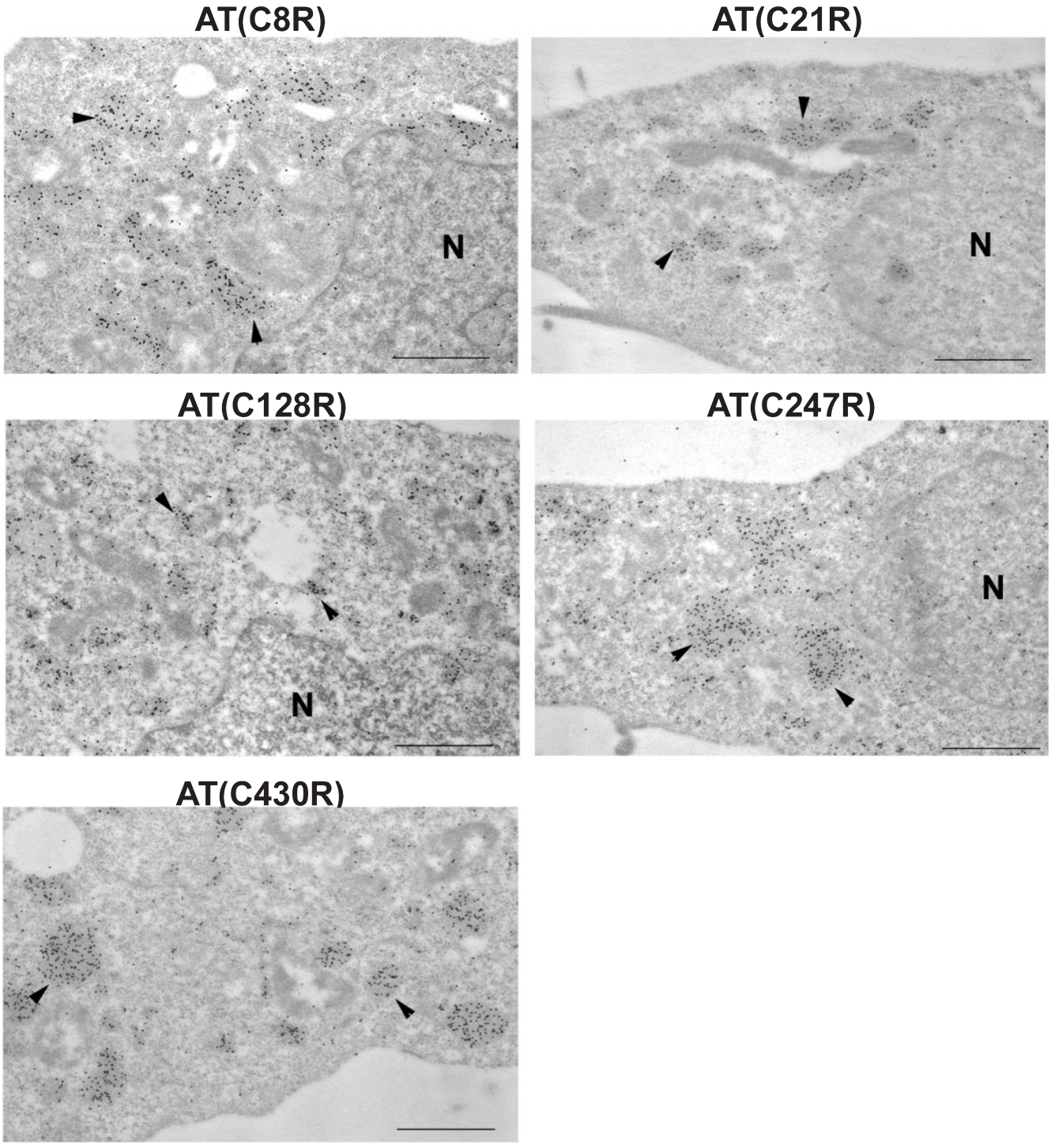

Fig. 4. **Immunoelectron micrographs of CHO cells overexpressing mutant ATs with a single mutation.** Immunogold staining was performed with anti-AT antibodies. Gold particles are present in variously sized membrane structures. The arrowheads indicate the typical structures accumulating mutant AT. Bar = 1 μm.

bly overexpressing mutant AT(C95R) (data not shown). On the other hand, the content of wild type AT in the cells did not increase so much since the AT was normally secreted into the medium during the incubation period of 72 h. The expression of ER chaperones in CHO cells expressing mutant AT(C95R) was compared to that in CHO cells expressing the wild type AT, since accumulation of misfolded proteins in the ER is known to induce the expression of several chaperones for quality control of secretory proteins (*32*, *33*). The contents of ER chaperones such as BiP and calnexin, however, did not increase in either cells expressing the wild type or mutant AT(C95R), suggesting that the unfolding protein response (UPR) was hardly induced in the cells.

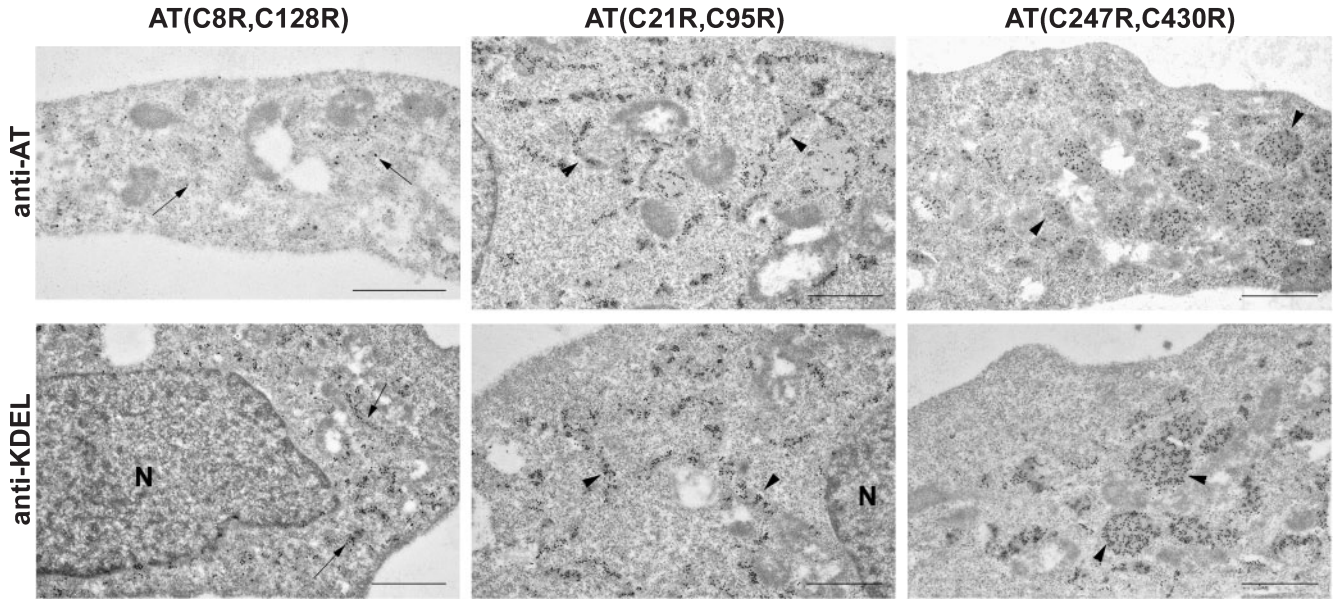

Fig. 5. **Immunoelectron micrographs of CHO cells overexpressing mutant ATs with a double mutation.** Immunogold staining was performed with anti AT antibodies (upper) or anti-KDEL antibodies (lower). In CHO cells overexpressing mutant AT(C21R,C95R) or AT(C247R,C430R), gold particles corresponding to AT are present in variously sized membrane structures (arrowheads). Gold particles corresponding to ER-resident proteins recognized by anti-KDEL antibodies are also present in similar structures (arrowheads). Arrows indicate gold particles corresponding to AT and the ER-resident proteins in CHO cells overexpressing mutant AT(C8R,C128R). Bar = 1 μm.

Next, we examined the localization of mutant AT(C95R) and RB-like structures by both immuno and transmission electron microscopy. As shown in Fig. 8A, gold particles corresponding to mutant AT(C95R) were detected at 18 h incubation and the number of gold particles was extremely increased at 36 h. The particles existed in the membranous structures that seem to comprise the ER, but they were not concentrated in the structures. After 72 h incubation with doxycycline, mutant AT(C95R) was observed in variously sized membranous structures, the largest structure being ~3 μm in diameter. We also examined the localization of ER-resident proteins bearing KDEL. Gold particles were detected in large sized structures resembling those accumulating mutant AT(C95R) (Fig. 8C), suggesting that the structures accumulating the mutant AT were derived from the ER. Interestingly, the number of dots did not increase in the cells and the concentration was decreased in the membranous structures (Fig. 8C). It was shown that the ER was well observed in CHO cells without the induction of mutant AT synthesis (Fig. 8B at 0 h). After 18 h incubation with doxycycline, swelling of the membranes was detected in several regions of the ER and the sizes of membranous structures had increased drastically at 36 h later. After the 72 h incubation, large ER structures as well as several small regions of the ER appeared (Fig. 8B). These results suggest that the accumulation of mutant AT(C95R) induces swelling of the ER. However, it has not yet determined whether or not mutant AT(C95R) accumulated in a specific compartment of the ER.

As a control experiment, we examined the localization of the wild type AT and the structure of the ER by immuno and transmission electron microscopy. CHO cells expressing the wild type AT neither accumulated at nor formed RB-like structures, and the morphology of ER did not change during the period after the induction of the wild type AT synthesis (data not shown).

DISCUSSION

In the process of protein maturation in secretory pathways, correct folding is important for normal secretion, acquisition of stability and physiological function. The formation of intra- or intermolecular disulfide bonds is one of the major posttranslational modification processes crucial for protein folding. Certain specific disulfide bonds play a key role(s) in protein folding and stabilization. For example, in the bovine pancreatic trypsin inhibitor (*34*), influenza virus hemagglutinin (*35*), the β-subunit of gastric H^+,K^+-ATPase (*36*), and insulin (*37*), the formation of the correct disulfide bonds is commonly thought to be important for efficient folding, stabilization, cell surface expression and secretion.

Roles of the Cysteine Residues and/or Disulfide Bonds of AT in Intracellular Accumulation and Formation of RB-Like Structures—AT contains six cysteine residues, which form three disulfide bonds (*3*, *4*). These disulfide bonds are, as a whole, thought to be essential for protein folding and for maintenance of the protease inhibitor function (*27*). To study further the role of each cysteine residue in both the accumulation of mutant AT and the formation of RB-like structures, we performed pulse-chase experiments and morphological analysis involving electron microscopy.

First, we found that the loss of each cysteine residue brought about a decrease in the secretion rate of the mutant AT (Fig. 2) as well as the formation of RB-like

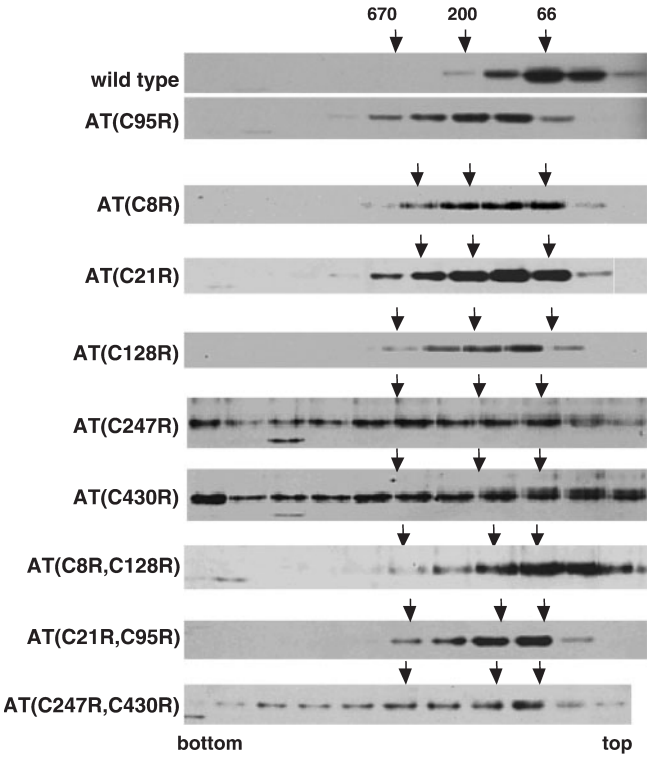

Fig. 6. **Sucrose gradient centrifugation of the wild type and mutant ATs.** CHO cells overexpressing the wild type and mutant ATs were incubated with 1 mM DSP, and excess DSP was inactivated by the addition of 50 mM glycine in PBS. The cells were lysed and the resulting lysates were centrifuged at 600 × *g* for 10 min, and then the supernatant fractions were subjected to the density gradient centrifugation as described under "EXPERIMENTAL PROCEDURES." An aliquot of each fraction obtained was separated by SDS-PAGE and subjected to immunoblot analysis. The molecular mass of each AT was calculated with reference to the molecular weights of standard proteins, *i.e.* bovine serum albumin (66 kDa), β-amylase (200 kDa), and thyroglobulin (670 kDa).

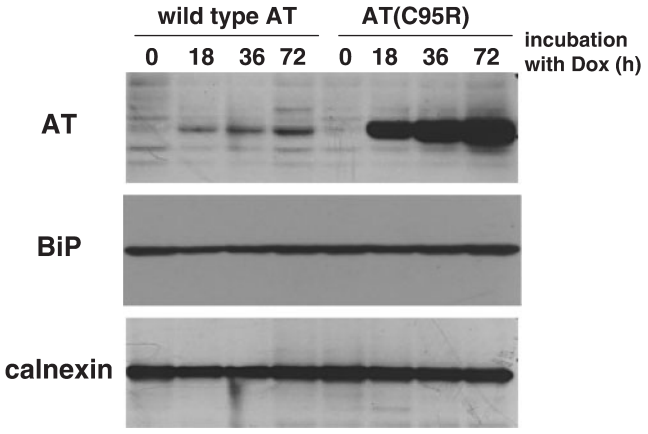

Fig. 7. **Immunoblot analysis of the wild type and mutant AT(C95R), BiP and calnexin in CHO cells in which expression of both ATs was controlled by the Tet-On system.** CHO cells transfected with pTRE2hyg/AT or AT(C95R) were cultured with doxycycline for different periods, and then the immunoblot analysis was performed as described under "EXPERIMENTAL PROCEDURES." In each lane, 150 μg (for AT) or 100 μg (for BiP and calnexin) of protein was applied.

structures (Fig. 4). There are several similarities in the cells expressing mutant ATs with single mutations, including AT(C95R) in the previous study. (i) Newly synthesized mutant ATs were hardly degraded in the cells and secreted only very slowly into the medium. Although the rate of secretion varied with each mutation, it showed first-order kinetics (Fig. 2). (ii) Most of the mutant ATs in the cells are suggested to possess the high mannose type of oligosaccharide (Fig. 2A) and probably accumulate in the ER. (iii) Wild type AT appeared to be a monomeric form on sucrose gradient centrifugation, whereas all mutant ATs with single mutations were dimeric or oligomeric forms (Fig. 6). (iv) The mutant ATs were found in variously sized membranous structures with a rather electron-dense morphology (Fig. 4). In addition, the dimeric forms of mutant ATs were detected on SDS-PAGE under non-reducing conditions, as in the case of mutant AT(C95R) (*27*) (data not shown). Therefore, all of the cysteine residues involved in disulfide bond formation are necessary for the correct folding of the AT molecule. Loss of any cysteine residue causes dimerization or oligomerization of the AT, and induces both the accumulation of AT in the ER and the formation of RB-like structures.

Previously, we found that mutant AT(C21R,C95R) with a double mutation was secreted faster than mutant AT(C95R) with a single mutation. This finding suggests that a free cysteine residue is responsible for the retention of AT in the ER, probably through an intermolecular disulfide bond (*27*). We had, therefore, expected that the mutant ATs with double mutations would be secreted faster than those with the corresponding single mutations. However, the fates of the mutant ATs revealed a different phenomenon. One mutant, AT(C8R,C128R), as expected, was indeed secreted faster than single mutations AT(C8R) and AT(C128R) (Fig. 3B). Furthermore, mutant AT(C8R,C128R) appeared mainly as a monomeric form on the sucrose gradient (Fig. 6), and did not accumulate in any membranous structures (Fig. 5). In contrast, the secretion of the other mutant, AT(C247R,C430R), was not improved compared to those of AT(C247R) and AT(C430R) (Figs. 2B and 3B). In addition, mutant AT(C247R,C430R) existed as a highly heterogeneous population (Fig. 6) and formed RB-like structures with a spherical shape (Fig. 5). Therefore, the disulfide bond between the cysteine residues at 247 and 430 seems to be critical for AT to have the correct conformation, and the absence of the disulfide bond causes aggregation of the mutant AT. In the cells expressing mutant AT(C21R,C95R), the secretion rate was higher than those of AT(C21R) and AT(C95R), but the rate was still lower by approximately 5 times than that of the wild type AT (Figs. 2B and 3B). It mainly existed as a dimeric form, and induced the formation of RB-like structures with a narrow and tubular shape (Fig. 5). The amount of AT(C21R,C95R) in the cells was less than those of AT(C21R) and AT(C95R) (data not shown), suggesting that the structure of the RB might be due to the difference in the accumulated amounts of AT in the cells. These results suggest that the responsibility of each

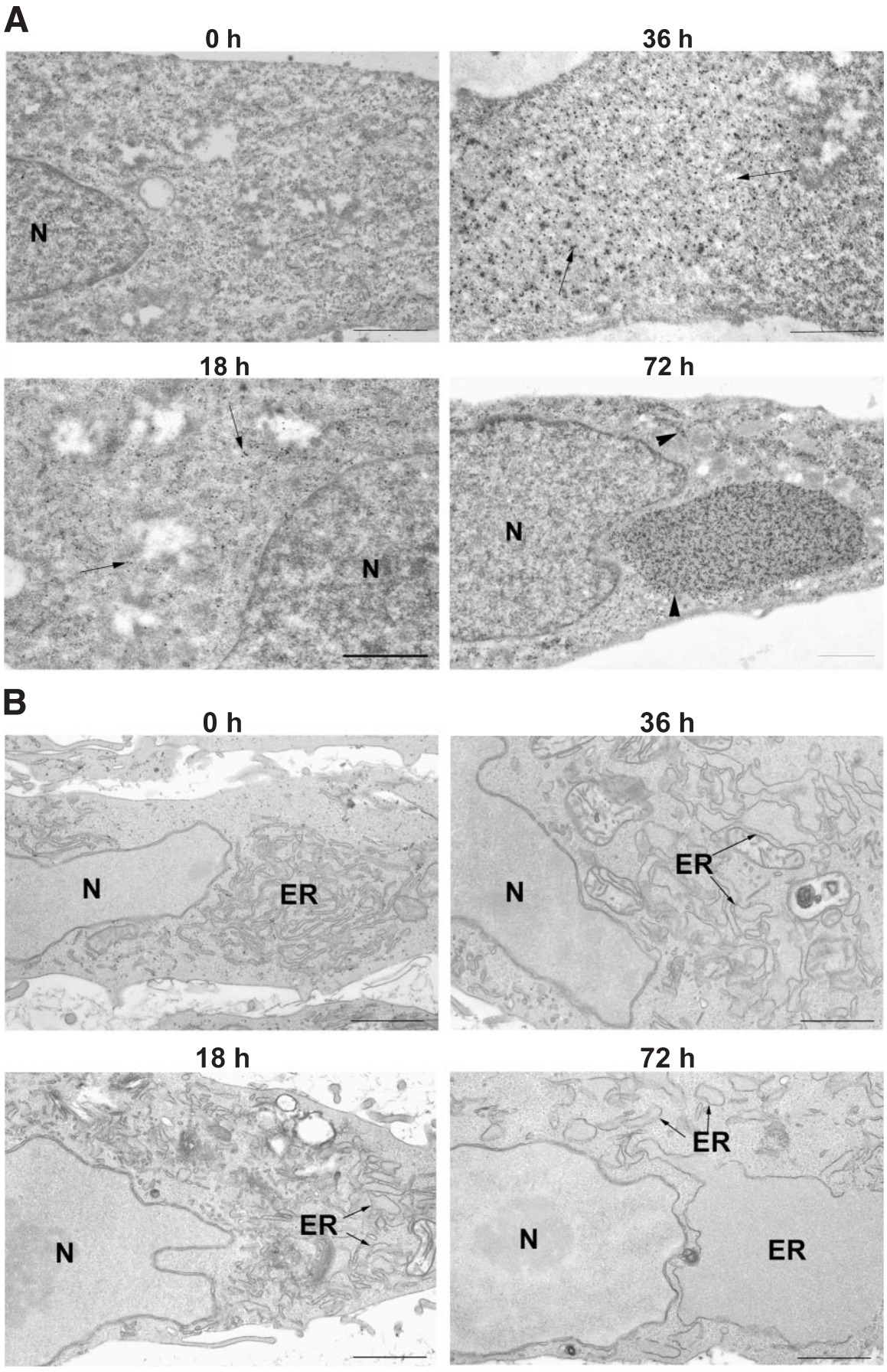

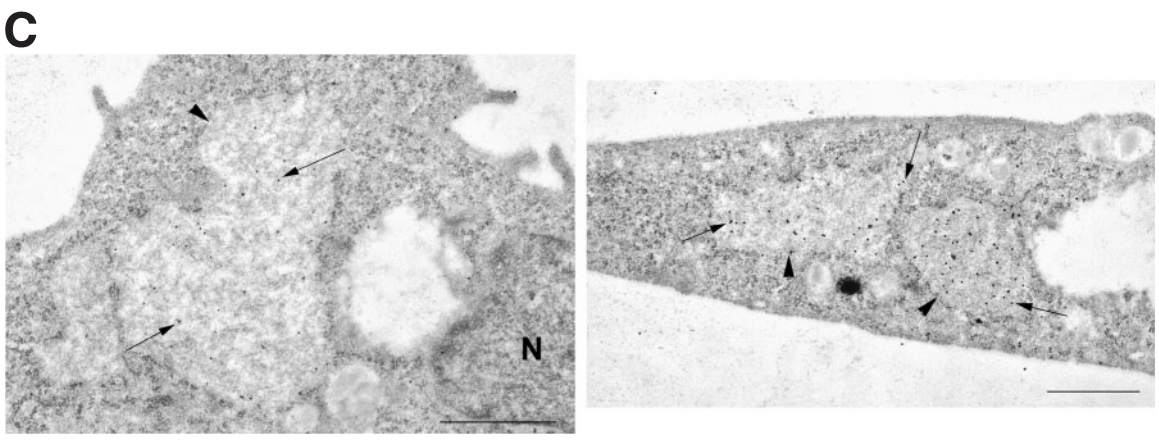

Fig. 8. **Immunoelectron and transmission electron micrographs of CHO cells in which expression of the wild type and mutant AT(C95R) was controlled by the Tet-On system.** A, immunogold staining of CHO cells overexpressing mutant AT(C95R) with anti-AT antibodies. Arrows indicate gold particles against AT in the CHO at 18 h and 36 h. Gold particles are present in an enormous membrane structure as well as small membrane structures (arrowheads) at 72 h. Bar = 1 μm. B, transmission electron microgram of CHO cells overexpressing mutant AT(C95R). The membrane structures corresponding to subregions of the ER (arrows) expanded during the expression of mutant AT(C95R) and an enormous ER structure appeared at 72 h. Bar = 1 μm. C, immunogold staining of CHO cells overexpressing mutant AT(C95R) with anti-KDEL antibodies at 72 h. Arrows indicate ER-resident proteins recognized by anti-KDEL antibodies. Gold particles are present in the induced membrane structures (arrowheads), and the structures are similar to those accumulating mutant AT(C95R). Bar = 1 μm.

disulfide bond for the accumulation of AT in the ER is different. The loss of the disulfide bond at residues 247–430 is the most critical for the secretion of AT. The disulfide bond at residues 247–430 exists in the protease-binding domain, which mainly consists of β-sheets, whereas those at residues 8–128 and 21–95 exist in the heparin-binding domain, which mainly consists of several α-helices (*5*, *7*). The loss of the 247–430 linkage would result in the release of the hydrophobic inside chains and make them liable to form aggregates. On the loss of the 8–128 linkage, on the other hand, the tertiary structure of the heparin binding domain would be maintained partially by the intact 21–95 linkage, and the absence of the 8–128 linkage would cause little damage since mutant AT(C8R,C128R) did not associate with BiP and was secreted faster than the other mutant ATs with single mutations. Dimerization and oligomerization through the free cysteine residues in AT molecules as well as through association with ER-resident proteins such as BiP (*27*) might prevent the AT from being sent back to the translocon composed of Sec 61 the degradation by proteasomes and also prevent the AT from exiting from the ER through exit sites into the Golgi apparatus.

Formation of RB-Like Structures—It is well known that the ER is capable of adjusting its size and architecture to adapt to changes in the environment. For example, overproduction of ER-resident membrane proteins such as HMG-CoA reductase (*38*, *39*), cytochrome b_5 (*40*, *41*), and aldehyde dehydrogenase (*42*) is known to induce conversion of the reticular ER into sheets of smooth ER called karmellae, or a whole or organized smooth ER. Recently, it was suggested that these structures are formed through weak homotypic interactions between the cytoplasmic domains of the overexpressed proteins (*41*). Expression of mutant Ste6p, a member of the ATP binding cassette (ABC) protein family, has been shown to induce a network of tubulo-vesiclar structures that seem to represent proliferated ER membranes in yeast (*43*). Similar structures called vesicular-tubular clusters have also been shown in the expression of mutant Pmp1a in yeast (*44*) and rubella virus E1 glycoprotein in the absence of the E2 subunit in mammalian cells (*45*). In addition, the overproduction of yeast Sec12p, a protein involved in COPII coat formation, inhibited ER and Golgi transport, and induced BiP bodies, punctate regions of the ER that accumulate Kar2p (*46*).

Here we examined the time course of RB formation by morphological analysis and uncovered the following characteristics of RB-like structures. (i) During the accumulation of a mutant AT, we found that subregions of the rough ER were dilated, their size increased, and thus finally a large expanded ER appeared (Fig. 8, A and B). These results suggest that the RB were originally the ER, and not structures that had budded from the ER. Wild type AT was secreted normally in spite of extensive synthesis of the AT. This excludes the possibility that mutant ATs accumulated in the ER lumen due to overflow of the traffic from the ER to the Golgi apparatus. In addition, the dilated membrane structures of the ER were never seen in the cells overexpressing wild type AT (data not shown). (ii) The structures of RB were very different from those observed in the cells overexpressing the various membrane proteins mentioned above. Accumulation of the proteins in the ER lumen does not seem to induce a network of ER membranes such as karmellae or vesicular-tubular clusters. (iii) The characteristics of RB are also different from those of the BiP bodies. Inhibition of ER-to-Golgi transport induces relocalization of BiP within the ER to form BiP bodies, where BiP, probably induced in the cells, is highly concentrated (*46*). On the other hand, in CHO cells overexpressing a mutant AT, ER-resident proteins such as BiP and GRP 94 were found not to be concentrated but to be rather diffuse in RB-like structures (Fig. 8C). In addition, the formation of the RB-

like structures does not seem to disturb normal secretory traffic from the ER since the secretion of newly synthesized proteins other than mutant ATs was normal (data not shown). Taken together, these findings suggest that RB are uniquely architected structures organized through expansion of the ER on the accumulation of misfolded proteins in the lumen and that RB are directly connected with the ER. In addition, the accumulation of misfolded proteins in the ER is well known to induce UPR (*32*, *33*). For example, mutant insulin(C96Y) with disruption of the intramolecular disulfide bond induced UPR (*47*), while CHO cells expressing mutant AT(C95R) did not (Fig. 7). Although how the signals from misfolded proteins are transmitted to the sensor molecules such as ATF6, IRE1α and IRE1β is not fully understood, it might involve the misfolded states of individual proteins in the ER.

In this study, we found that (i) the correct folding of each disulfide bond is essential for the normal secretion of AT. (ii) Mutation of each cysteine residue of AT or loss of the disulfide bonds between cysteine residues 21–95 and 247–430 resulted in the mutant AT being retained for a long time in the ER without being degraded. (iii) The oligomerization of a mutant AT caused by impaired disulfide bond formation induced the formation of RB-like structures, which are probably connected with the ER. The precise mechanism by which RB-like structures are formed and the dynamics of RB-like structures in these cells will be the subjects of future research.

This research was supported in part by the Ministry of Education, Science, Sports and Culture of Japan (13877372 and 15659017 to TI, and 13671054 to TO). We would also like to acknowledge Pacific Edit for reviewing the manuscript prior to submission for publication.

REFERENCES

1. Travis, J. and Salvesen, G.S. (1983) Human plasma proteinase inhibitors. *Annu. Rev. Biochem.* **52**, 655–709
2. Björk, I. and Olson, S.T. (1997) Antithrombin. A bloody important serpin. *Adv. Exp. Med. Biol.* **425**, 17–33
3. Petersen, T.E., Dudek-Wojciechowska, G., Sottrup-Jensen, L., and Magnusson, S. (1979) Primary structure of antithrombin III (heparin cofactor). Partial homology between α_1-antitrypsin and antithrombin III in *The Physiological Inhibitors of Blood Coagulation and Fibrinolysis* (Collen, D., Wiman, B., and Verstraete, M., eds.) pp. 43–54, Elsevier Science Publisher B.V., Amsterdam
4. Bock, S.C., Wion, K.L., Vehar, G.A., and Lawn, R.M. (1982) Cloning and expression of the cDNA for human antithrombin III. *Nucleic Acids Res.* **10**, 8113–8125
5. Sun, X.J. and Chang, J.Y. (1989) Heparin binding domain of human antithrombin III inferred from the sequential reduction of its three disulfide linkages. An efficient method for structural analysis of partially reduced proteins. *J. Biol. Chem.* **264**, 11288–11293
6. Chandra, T., Stackhouse, R., Kidd, V.J., and Woo, S.L.C. (1983) Isolation and sequence characterization of a cDNA clone of human antithrombin III. *Proc. Natl Acad. Sci. USA* **80**, 1845–1848
7. Skinner, R., Abrahams, J.P., Whisstock, J.C., Lesk, A.M., Carrell, R.W., and Wardell, M.R. (1997) The 2.6 Å structure of antithrombin indicates a conformational change at the heparin binding site. *J. Mol. Biol.* **266**, 601–609
8. Mille, B., Watton, J., Barrowcliffe, T.W., Mani, J.C., and Lane, D.A. (1994) Role of N- and C-terminal amino acids in antithrombin binding to pentasaccharide. *J. Biol. Chem.* **269**, 29435–29443
9. Thaler, E. and Lechner, K. (1981) Antithrombin III deficiency and thromboembolism. *Clin. Hematol.* **10**, 369–390
10. Lane, D.A., Bayston, T., Olds, R.J., Fitches, A.C., Cooper, D.N., Millar, D.S., Jochmans, K., Perry, D.J., Okajima, K., Thein, S.L., and Emmerich, J. (1997) Antithrombin mutation database: 2nd (1997) update. *Thromb. Haemostasis* **77**, 197–211
11. Fra, A.M., Fagioli, C., Finazi, D., Sitia, R., and Alberini, C.M. (1993) Quality control of ER synthesized proteins: an exposed thiol group as a three-way switch mediating assembly, retention and degradation. *EMBO J.* **12**, 4755–4761
12. Ellgaard, L., Molinari, M., and Helenius, A. (1999) Setting the standards: quality control in the secretory pathway. *Science* **286**, 1882–1888
13. Ellgaard, L., and Helenius, A. (2003) Quality control in the endoplasmic reticulum. *Nat. Rev. Mol. Cell. Biol.* **4**, 181–191
14. Aridor, M., and Balch, W.E. (1999) Integration of endoplasmic reticulum signaling in health and disease. *Nat. Med.* **5**, 745–751
15. Wiertz, E.J.H.J., Tortorella, D., Bogyo, M., Yu, J., Mothes, W., Jones, T.R., Rapoport, T.A., and Ploegh, H.L. (1996) Sec61-mediated transfer of a membrane protein from the endoplasmic reticulum to the proteasome for destruction. *Nature* **384**, 432–438
16. Wickner, S., Maurizi, M.R., and Gottesman, S. (1999) Post-translational quality control: folding, refolding, and degrading proteins. *Science* **286**, 1888–1893
17. Tokunaga, F., Shirotani, H., Hara, H., Kozuki, D., Omura, S., and Koide, T. (1997) Intracellular degradation of secretion defect-type mutants of antithrombin is inhibited by proteasomal inhibitors. *FEBS Lett.* **412**, 65–69
18. Tokunaga, F., Hara, K., and Koide, T. (2003) N-Linked oligosaccharide processing, but not association with calnexin/calreticulin is highly correlated with endoplasmic reticulum-associated degradation of antithrombin Glu313-deleted mutant. *Arch. Biochem. Biophys.* **411**, 235–242
19. Kopito, R.R. (2000) Aggresomes, inclusion bodies and protein aggregation. *Trends Cell Biol.* **10**, 524–530
20. Schweitzer, P.A., Tayor, S.E., and Shultz, L.D. (1991) Synthesis of abnormal immunoglobulins by hybridomas from autoimmune "viable motheaten" mutant mice. *J. Cell Biol.* **114**, 35–43
21. Valetti, C., Grossi, C.E., Milstein, C., and Sitia, R. (1991) Russell bodies: a general response of secretory cells to synthesis of a mutant immunoglobulin which can neither exit from, nor be degraded in, the endoplasmic reticulum. *J. Cell Biol.* **115**, 983–994
22. Lomas, D.A., Evans, D.L., Finch, J.T., and Carrell, R.W. (1992) The mechanism of Z α_1-antitrypsin accumulation in the liver. *Nature* **357**, 605–607
23. Carlson, J.A., Rogers, B.B., Sifers, R.N., Hawkins, H.K., Finegold, M.J., and Woo, S.L. (1988) Multiple tissues express α_1-antitrypsin in transgenic mice and man. *J. Clin. Invest.* **82**, 26–36
24. Carlson, J.A., Rogers, B.B., Sifers, R.N., Finegold, M.J., Clift, S.M., DeMayo, F.J., Bullock, D.W., and Woo, S.L. (1989) Accumulation of PiZ α1-antitrypsin causes liver damage in transgenic mice. *J. Clin. Invest.* **83**, 1183–1190
25. Umebayashi, K., Hirata, A., Fukuda, R., Horiuchi, H., Ohta, A., and Takagi, M. (1997) Accumulation of misfolded protein aggregates leads to the formation of Russell Body-like dilated endoplasmic reticulum in yeast. *Yeast* **13**, 1009–1020
26. Ozawa, T., Takikawa, Y., Niiya, K., Fujiwara, T., Suzuki, K., Sato, S., and Sakuragawa, N. (1997) Antithrombin Morioka (Cys95-Arg): a novel missense mutation causing type I antithrombin deficiency. *Thromb. Haemostasis* **77**, 403
27. Tanaka, Y., Ueda, K., Ozawa, T., Sakuragawa, N., Yokota, S., Sato, R., Okamura, S., Morita, M., and Imanaka, T. (2002) Intracellular accumulation of antithrombin *Morioka* (C95R), a novel mutation causing type I antithrombin deficiency. *J. Biol. Chem.* **277**, 51058–51067.

28. Imanaka, T., Aihara, K., Takano, T., Yamashita, A., Sato, R., Suzuki, Y., Yokota, S., and Osumi, T. (1999) Characterization of the 70-kDa peroxisomal membrane protein, an ATP binding cassette transporter. *J. Biol. Chem.* **274**, 11968–11976
29. Yokota, S., Kamijo, K., and Oda, T. (2000) Aggregate formation and degradation of overexpressed wild-type and mutant urate oxidase proteins. Quality control of organelle-destined proteins by the endoplasmic reticulum. *Histochem. Cell Biol.* **114**, 433–446
30. Urade, R., Kusunose, M, Moriyama, T., Higasa, T., and Kito, M. (2000) Accumulation and degradation in the endoplasmic reticulum of a truncated ER-60 devoid of C-terminal amino acid residues. *J. Biochem.* **127**, 211–220
31. Kashiwayama, Y., Morita, M., Kamijo, K., and Imanaka, T. (2002) Nucleotide-induced conformational changes of PMP70, an ATP binding cassette transporter on rat liver peroxisomal membranes. *Biochem. Biophys. Res. Commun.* **291**, 1245–1251
32. Mori, K. (2000) Tripartite management of unfolded proteins in the endoplasmic reticulum. *Cell* **101**, 451–454
33. Reimertz, C., Kögel, D., Rami, A., Chittenden, T., and Prehn, J.H.M. (2003) Gene expression during ER stress-induced apoptosis in neurons: induction of the BH3-only protein Bdc3/PUMA and activation of the mitochondrial apoptosis pathway. *J. Cell Biol.* **162**, 587–597
34. Kowalski, J.M., Parekh, R.N., and Wittrup, K.D. (1998) Secretion efficiency in *Saccharomyces cerevisiae* of bovine pancreatic trypsin inhibitor mutants lacking disulfide bonds is correlated with thermodynamic stability. *Biochemistry* **37**, 1264–1273
35. Segal, M.S., Bye, J.M., Sambrook, J.F., and Gething, M.J. (1992) Disulfide bond formation during the folding of influenza virus hemagglutinin. *J. Cell Biol.* **118**, 227–244
36. Kimura, T., Tabuchi, Y., Takeguchi, N., and Asano, S. (2002) Mutational study on the roles of disulfide bonds in the β-subunit of gastric H^+, K^+-ATPase. *J. Biol. Chem.* **277**, 20671–20677
37. Wang, J., Takeuchi, T., Tanaka, S., Kubo, S., Kayo, T., Lu, D., Takata, K., Koizumi, A., and Izumi, T. (1999) A mutation in the insulin 2 gene induces diabetes with severe pancreatic β-cell dysfunction in the *Mody* mouse. *J. Clin. Invest.* **103**, 27–37
38. Pathak, R.K., Luskey, K.L., and Anderson, R.G., (1986) Biogenesis of the crystalloid endoplasmic reticulum in UT-1 cells: evidence that newly formed endoplasmic reticulum emerges from the nuclear envelope. *J. Cell Biol.* **102**, 2158–2168
39. Profant, D.A., Roberts, C.J., Koning, A.J., and Wright, R.L. (1999) The role of the 3-hydroxy 3-methylglutaryl coenzyme A reductase cytosolic domain in *Karmellae* biogenesis. *Mol. Biol. Cell* **10**, 3409–3423
40. Vergeres, G., Yen, T.S.B., Aggeler, J., Lausier, J., and Waskell, L. (1993) A model system for studying membrane biogenesis. Overexpression of cytochrome b_5 in yeast results in marked proliferation of the intracellular membrane. *J. Cell Sci.* **106**, 249–259
41. Snapp, E.L., Hegde, R.S., Francolini, M., Lombardo, F., Colombo, S., Pedrazzini, E., Borgese, N., and Lippincott-Schwartz, J. (2003) Formation of stacked ER cisternae by low affinity protein interactions. *J. Cell Biol.* **163**, 257–269
42. Yamamoto, A., Masaki, R., and Tashiro, Y. (1996) Formation of crystalloid endoplasmic reticulum in COS cells upon overexpression of microsomal aldehyde dehydrogenase by cDNA transfection. *J. Cell Sci.* **109**, 1727–1738
43. Huyer, G., Longsworth, G.L., Mason, D.L., Mallampalli, M.P., McCaffery, J.M., Wright, R.L., and Michaelis, S. (2004) A striking quality control subcompartment in *Saccharomyces cerevisiae*: The endoplasmic reticulum-associated compartment. *Mol. Biol. Cell* **15**, 908–921
44. Ferreira, T., Mason, A.B., Pypaert, M., Allen, K.E., and Slayman, C.W. (2002) Quality control in the yeast secretory pathway. A misfolded Pma1 H^+-ATPase reveals two checkpoints. *J. Biol. Chem.* **277**, 21027–21040
45. Hobman, T.C., Woodward, L., Farquhar, M.G., (1992) The rubella virus E1 glycoprotein is arrested in a novel post-ER, pre-Golgi compartment. *J. Cell Biol.* **118**, 795–811
46. Nishikawa, S., Hirata, A., and Nakano, A. (1994) Inhibition of endoplasmic reticulum (ER)-to-Golgi transport induces relocalization of binding protein (BiP) within the ER to form the BiP bodies. *Mol. Biol. Cell* **5**, 1129–1143
47. Oyadomari, S., Koizumi, A., Takeda, K., Gotoh, T., Akira, S., Araki, E., and Mori, M. (2002) Targeted disruption of the *Chop* gene delays endoplasmic reticulum stress-mediated diabetes. *J. Clin. Invest.* **109**, 525–532